JET–P(92)67

J.P. Coad, B. Farmery, J. Linke, E. Wallura
and JET Team

# Experience with Boron-Carbide Coated Target Tiles in JET

# Experience with Boron-Carbide Coated Target Tiles in JET

J.P. Coad, B. Farmery[1], J. Linke[2], E. Wallura[2] and JET Team*

*JET-Joint Undertaking, Culham Science Centre, OX14 3DB, Abingdon, UK*

[1]*University of Sussex, Brighton, Sussex, BN1 9QH, UK*
[2]*Forschungszentrum Jiilich GmbH, D-5170 Jiilich, Germany*
*\* See Annex*

# EXPERIENCE WITH BORON-CARBIDE COATED TARGET TILES IN JET

J.P. Coad, B. Farmery*, J. Linke+ and E. Wallura+

JET Joint Undertaking, Abingdon, Oxon, OX14 3EA, UK

*University of Sussex, Brighton, Sussex, BN1 9QH, UK

+Forschungszentrum Jülich GmbH, D-5170 Jülich, FRG

## ABSTRACT

Three graphite tiles coated with $B_4C$ were mounted in the X-point strike region of JET during operations in 1991. The coatings remained adherent, though areas reached temperatures at which local melting occurred. Boron and deuterium analyses in the area surrounding the tiles suggest sublimation of boron was an important release mechanism, and that the region between the strike zones (the private flux region) is a major redeposition area.

## INTRODUCTION

In recent years the development of low-Z materials for plasma-facing components (PFC's) has progressed beyond the all-carbon first wall to include the even lighter elements boron and beryllium. JET has evaporated Be over the first wall and operated with a mixture of Be and carbon PFC's[1], whilst many other tokamaks have incorporated boron in the first wall either from gaseous sources[2] or by using B-C composite components[3]. One method of introducing boron being investigated is the use of $B_4C$ - coated components[4], which offers the possibility of in-situ refurbishing of eroded components by plasma spraying. Three $B_4C$ - coated tiles were included in the upper X-point strike area of JET during 1991, and the post-mortem analysis of these tiles is described below.

However, the $B_4C$ coatings were included in JET not as a material test, but to provide a source element (boron) to study redeposition in the divertor channel. Modelling of erosion and redeposition in divertors is of vital importance for the ITER design[5], and any experimental information may be useful in developing or validating theoretical models. Erosion at the JET X-point plates at the time of the exposure of the $B_4C$ coatings was very variable, and the results are the culmination of about 370 X-point discharges. Nevertheless, the analyses give some interesting pointers to transport phenomena in the divertor channel.

## EXPERIMENTAL

### (1)  Coating the tiles with B₄C

The upper X-point tiles were made of Aerolor graphite, and were coated by low pressure plasma spraying at the Technical University of Aachen (RWTH). Three tiles were sprayed with $B_4C$ in a single pass to produce a coating approximately 70μm thick. Analysis by scanning electron microscopy (SEM) revealed ~2% of metals (Ni, Cr, Fe) as a surface contamination, which was believed to be due to pickup of impurities in the powder feed hopper. The impurity level was reduced to ~0.3% by sand-blasting the surface with $B_4C$ particles.

### (2)  Mounting and plasma exposure in JET

Figure 1 shows a layout of tiles on a section of the roof of the JET torus. The three coated tiles (indicated by hatching) form a poloidal set across the regions of maximum plasma-surface interaction for X-point discharges (the "strike zones"). The position of the tiles in relation to the vessel cross-section (and the plasma during the so-called "X-point" phase) is shown in Figure 2. The tiles are mounted on separate plates for each of the 40 sectors of the vessel, to avoid bridging the bellows which increase the resistivity of the torus. The breaks between sectors are indicated by slight gaps in the plan (Figure 1). The central sector of each octant (C) is covered by two plates, and there is a small gap (also shown in Figure. 1) between them: the $B_4C$ - coated tiles were at the edge of this central space. A problem with this design of wall protection was that slight misalignments between sectors (or even between tiles on a plate) resulted in high heat loads (hot spots) at raised edges because the plasma is incident at ~2° to horizontal. Many of the sector joints evinced such hot spots. For normal magnetic field configurations the plasma forms a hot spot to the left of a break (in Figure 1) at the outer strike point or to the right of the break at the inner strike point. A number of discharges were also run with either reversed field or reversed plasma current. The $B_4C$-coated tile at the outer strike point (SC47) was severely eroded midway along its edge adjacent to the sector break (other tiles showing some erosion were SC7 and SC15 [right side] and SC12, SC13 and SC43 [left side]).

The tiles were present during operations in JET from June to August 1992. (In September a redesigned set of carbon-fibre-reinforced graphite tiles were installed). 370 discharges with X-point phases were run during this period, the X-

point phases usually lasting about 5 secs (interaction between the plasma and the tiles during limiter discharges, and during the limiter phases of X-point discharges is much less and can be disregarded). There were 37 sessions of Be-evaporation spread throughout the period, during which a total of approximately $1.5 \times 10^{18}$ Be atoms $cm^{-2}$ is estimated to have been deposited over these X-point tiles.

(3)    Ion Beam Analysis (IBA) and Scanning Electron Microscopy (SEM)

Following their removal from the torus, the tiles were examined using the ion beam analysis techniques Rutherford backscattering (RBS), proton induced X-ray emission (PIXE) and Nuclear Reaction Analysis (NRA). The combination of these techniques allowed all elements  present in the  outer few microns of the tile surfaces to be determined.   In particular the NRA reactions $^{11}B(p, \alpha)\,^{8}Be$ using 0.7 MeV protons, and $^{12}C\,(^{3}He, p)\,^{14}N$, $^{9}Be\,(^{3}He, p)\,^{11}B$ and $^{2}D\,(^{3}He, p)\,^{4}He$ using 2.5MeV $^{3}He$ ions were used to quantify B, C, Be and D in the outermost $1\mu m$ (approx).  The area of analysis (beam size) is 1mm diameter.

After IBA the tiles were examined in an SEM fitted with energy-dispersive X-ray analysis (EDX).  In order to avoid contaminating the SEM with beryllium, the tiles were first washed with a proprietary detergent (tiles SC44 and SC47) and distilled water (all three tiles).  The tiles were baked in the SEM vacuum system to 80°C for 12 hours before analysis.  The beam size in the SEM is $<0.1\mu m$,  but the EDX analyses have all been taken from areas between 10 x $10\mu m$ and 100 x $100\mu m$ (depending on the raster size) and are of the outermost $1\mu m$ (approx).

RESULTS

Analysis of the $B_4C$ coated tiles after exposure in JET on the millimetre scale (IBA) showed that the coating was intact everywhere though the boron count was reduced by about a factor of ten near the edges of the tiles likely to be eroded by the plasma.   The higher spatial resolution of the SEM reveals a more complicated picture.   The $B_4C$ coating is generally intact and appears to be overlaid by a smoother deposit which has a widespread network of cracks ("crazing"), the individual islands so formed being typically 200-500$\mu m$ in diameter as is clearly seen in Figure 3 which is a secondary electron image from near the centre of tile SC47.  Also shown in Figure 3 is an area without the crazed appearance with a rounded feature on its right.  Figure 4 shows a somewhat similar area from the centre of SC47, this time the image being formed by back-scattered electrons (BSE).  This BSE image demonstrates more clearly that the

agglomerations are due to film melting. (The crazing of the film over the unmelted areas which is similar to that in Figure 3 is not as obvious in the BSE image). Localized melt regions are widespread over SC47 but have not been observed on SC39 or SC44. EDX analyses (using a windowless detector) have been taken from many points on each tile, the low energy region of two from the areas indicated on Figure 3 being given in Figure 5. The melt droplet was rich in boron (as was invariably the case from such areas) whilst away from the melt area the spectrum shows predominantly carbon and oxygen. The carbon to oxygen ratios recorded from the tiles from unmelted regions vary considerable, with sometimes a shoulder on the carbon peak indicating some boron. It should be noted that there may be significant beryllium concentrations near the surface (Be is undetectable by EDX), and this may account for variations in the oxygen levels.

Melting of $B_4C$ coatings has been observed at substrate temperatures of $2100°C$ and above[4]: this is lower than the melting point for solid $B_4C$ of $2400°C$ probably due to imperfect thermal contact between coating and substrate. SC 47 is likely to have been the hottest of the three tiles and has clearly been approaching the melting temperature on occasions. The variable ratio of boron to carbon may reflect differences in the thickness of the overlying layer of material redeposited by the plasma which will contain principally C, Be and deuterium, and by analogy with deposits in all-carbon machines may be referred to as $\alpha$-Be/C:H/D.

During X-point discharges boron (and carbon) will have been sputtered (and perhaps evaporated) from the $B_4C$ - coated tiles (particularly from the edges of SC47 and SC39, and from larger areas at the start of the campaign before most of the surfaces were covered by redeposition from the plasma). After travelling a short distance the sputtered atoms will be ionised, entrained in the particle flux along the field lines and redeposited some distance away from the source point. A number of the surrounding tiles have been surveyed for boron, and selected results are shown in Figure 6 and 7. Figure 6 gives the boron counts recorded from points on a toroidal line across sector VIII C passing through the centre of SC39 (and thus between the two strike zones). Figure 7 shows data from analyses along two poloidal survey lines, their positions relative to the coated tiles being shown on Figure 1. Analyses close to tile edges are frequently out of line with analyses on the flat surfaces nearby due to the different flux density on the curved edges, which sometimes leads to erosion and sometimes extra deposition, so should be disregarded. The symmetry in Figure 6 is consistent with the right-hand edge of SC39 (and SC47) acting as source, and transport in either toroidal direction being equally probable. The folding length for the (final) redeposition

4

is of the order of 100mm.  Figure 7 shows that most of the boron is redeposited in the private flux region between the strike zones, and is not  peaked along the lines of the strike zones (or in the plasma scrape-off-layers (SOL)).

A survey of deuterium concentrations obtained by NRA has also been made over the tiles.   Deuterium is co-deposited with carbon and to a first approximation indicates the amount of carbon redeposited in that area. However, deuterium concentrations within  plasma deposits can be reduced by heating the substrates to high temperatures, so tiles exhibiting erosion may be expected to have lower deuterium levels.  Within this sector tiles SC13, SC43, SC7, SC15 and SC47 fall within this category and on these tiles the D concentration was generally $<10^{18}$ atoms $cm^{-2}$ and in some areas $<10^{17}$ atoms $cm^{-2}$.  Of the remaining tiles, SC45 has the lowest average D concentration, which apart from points close to the edge, averages $\sim 8 \times 10^{17}$ atoms $cm^{-2}$.  Tiles SC37, SC38, SC39 and SC9 (between the strike zones) average $4.0 \times 10^{18}$, $1.7 \times 10^{18}$, $2.8 \times 10^{18}$ and $3.0 \times 10^{18}$ atoms $cm^{-2}$ (respectively).  The inner row of tiles SC42, SC44 and SC14 average $6.1 \times 10^{18}$, $5.2 \times 10^{18}$ and $4.0 \times 10^{18}$ atoms $cm^{-2}$, whilst a poloidal scan on SC12, despite there being some erosion elsewhere on the tile, averaged $6.1 \times 10^{18}$ atoms $cm^{-2}$ .   These NRA analyses refer to the outermost $1\mu m$ (approx).  However, it is clear from the spectra and from other analyses that for levels much above $10^{18}$ atoms $cm^{-2}$ the actual D concentrations are underestimated, because the redeposited films are clearly thicker than 1 $\mu m$ (but there is little contribution from the inner part of the film to the NRA signal).

Although these D analyses are variable due to irregularities in tile positioning etc, there is a clear trend of increasing D level towards decreasing plasma radius. At and beyond the outer strike point the D levels are relatively low, with all the thicker layers being in the private zone or at the inner strike zone.

DISCUSSION

The $B_4C$ coating exposed in JET remained adherent after ~370 pulses (with attendant thermal cycling).  Local melting occurred on one tile, suggesting that this tile probably reached ~2000°C during high power X-point discharges.  Due to the mounting system and tile design used at this time, many tiles in the X-point region were slightly prominent  (generally at sector joints but randomly distributed) and received much higher fluxes.  Temperatures in excess of 2000°C were not unusual for such tiles and although these coated tiles were not in the field of view of any of the viewing cameras, it is quite possible that SC47 reached such temperatures.

The distribution of boron in the areas surrounding the coated tiles was unexpected. The predication[5] from the linked kinetic and Monte Carlo codes of Brooks[6] is that atoms sputtered from the divertor plates will, once ionised, travel along field lines to be redeposited. Since the angle of incidence toroidally (~2°) is much less than the poloidal angle of incidence to the target (~45°), the majority of the movement is toroidal and downstream from the sputtering point. This is not important for a toroidally uniform source (eg. carbon from graphite targets), but is relevant for a discrete source.

Densities at the JET divertor separatrix (~ $10^{19}m^{-3}$[7]) are one to two orders of magnitude less than those predicted for ITER, so that the ionisation path length for sputtered atoms in JET is of the order of centimetres rather than millimetres or less in ITER. It may be, therefore, that boron sputtered at near-normal directions from the strike zones can travel toroidally out of the sector before returning along the field lines to the target surface and is not detected. Boron atoms sputtered at large angles from the normal to the surface may either be ionised within the private flux region and return to the surface within the area surveyed, or in the other direction travel poloidally out of the area surveyed. Most transport should be <u>away</u> from the private zone, due to the angle of the field lines to the target plate, and this effect should dominate over the random angle of sputtering [5].

Although tiles from outside the area analysed are not available to check for boron, the fine details of the B redeposition seen do not fit comfortably with the above suggestions. Firstly, the shape of the fall-off in B toroidally (figure 6) is not that to be expected if most boron is travelling out of the sector. Furthermore, the largest amount of redeposited boron observed (on SC7) is up to 7.6% of the boron signal from a B₄C coating standard and ~ 14% of the average recorded from flat regions of the exposed, coated tiles SC39, SC44 and SC47. (The lower B levels on these tiles may be due to the overlaying deposits and/or selective loss of boron during operations). These percentages suggest one is seeing the major redeposition sites rather than the statistical tail of the distribution. The deuterium distribution also suggests that the private zone is a major redeposition site. Redeposition remains large in line with the inner strike zone, but this strike zone can on occasions be located on the tile inboard of the three analysed tiles, so the fall-off in D may be just starting. If the transport mechanisms outlined above dominated, then the largest deposition should occur in the SOL beyond the strike zones, but this does not appear to be the case.

A partial explanation for the above inconsistencies may be that the dominant mechanism causing boron to leave the surface is sublimation. Atoms emitted thermally have kinetic energies 2-3 orders of magnitude lower than sputtered atoms, so ionisation will take place much closer to the source, and the deposition profile in figure 7 would be understandable. Sublimation of carbon is believed to be occurring at the hot spots during the carbon blooms frequently observed using these tiles [8]. Since sublimation of boron occurs at lower temperatures than for carbon, it is likely that it occurred at the edges of SC47 and SC39. It is not clear that sublimation rather than sputtering sources will effect the poloidal distribution of boron or deuterium. However, further analyses will be carried out over a larger poloidal range, and modelling techniques will be used to compare transport of sublimed rather than sputtered atoms with the complete experimental data set.

## CONCLUSIONS

Three $B_4C$ - coated tiles were used in the X-point target region of JET during operations in 1991. The coating remained adherent, but localised melting occurred in small areas over one of the tiles which is believed to have regularly reached temperatures of the order of 2000°C.

The amount of boron redeposition on other tiles in the sector of the vessel containing the coated tiles have been mapped. The toroidal plot of the redeposition shows a short mean free path which is more consistent with sublimation of boron from the source tiles than sputtering.

Poloidal plots of the redeposition of boron in the sector are clearly peaked in the private zone between the plasma strike points. The expected peaks in redeposition outside the strike zones were not observed, but may have been missed by being beyond the region analysed. However, the amount of deuterium trapped by redeposition from the plasma within the sector is also peaked within the private zone. These analyses will be continued to provide a more complete data set for modelling which is of clear relevance to the future JET divertor operation and to ITER.

## REFERENCES

[1]   P R Thomas and the JET Team, J Nuclear Materials <u>176 and 177</u> (1990) 3.

[2]   J Winter, H-G Esser, H Reimer, L Grobusch, J von Seggern and P Wienhold, J Nuclear Materials <u>176 and 177</u> (1990) 486.

[3]   C Boucher, F Martin, B L Stansfield, B Terrault, the TdeV Team, Y Hirooka, B Conn, T Matsuda, J Winter and H G Esser, Proc 10th Plasma Surface Interactions Conference, Monterey, USA, March 1992 (to be published in J Nuclear Materials).

[4]   S Deschka, J Linke, H Nickel and E Wallura, Fusion Engineering and Design <u>18</u> (1991) 157.

[5]   S A Cohen, R F Mattas and K A Werley, Princeton Plasma Physics Laboratory report PPPL-2823 (Feburary 1992) (available from National Technical Information Service, Springfield, Va 22161, USA).

[6]   J Brooks, J Nuclear Materials <u>170</u> (1990) 164.

[7]   J A Tagle, S Clement, A Loarte, L de Kock, P J Harbour, D O'Brien, S K Erents, G Janeschitz, C Nicholson and J Vince, Proc 10th Plasma Surface Interactions Conference, Monterey, USA, March 1992 (to be published in J Nuclear Materials).

[8]   C G Lowry, W N Ady, D J Campbell, P Carman, S Clement, E B Deksnis, A Gondhalekar, P J Harbour, L Horton, G Janeschitz, M Lesourd, J Lingertat, M A Pick, G Saibene, D D R Summers and P R Thomas, Proc 10th Plasma Surface Interactions Conference, Monterey, USA, March 1992 (to be published in J Nuclear Materials).

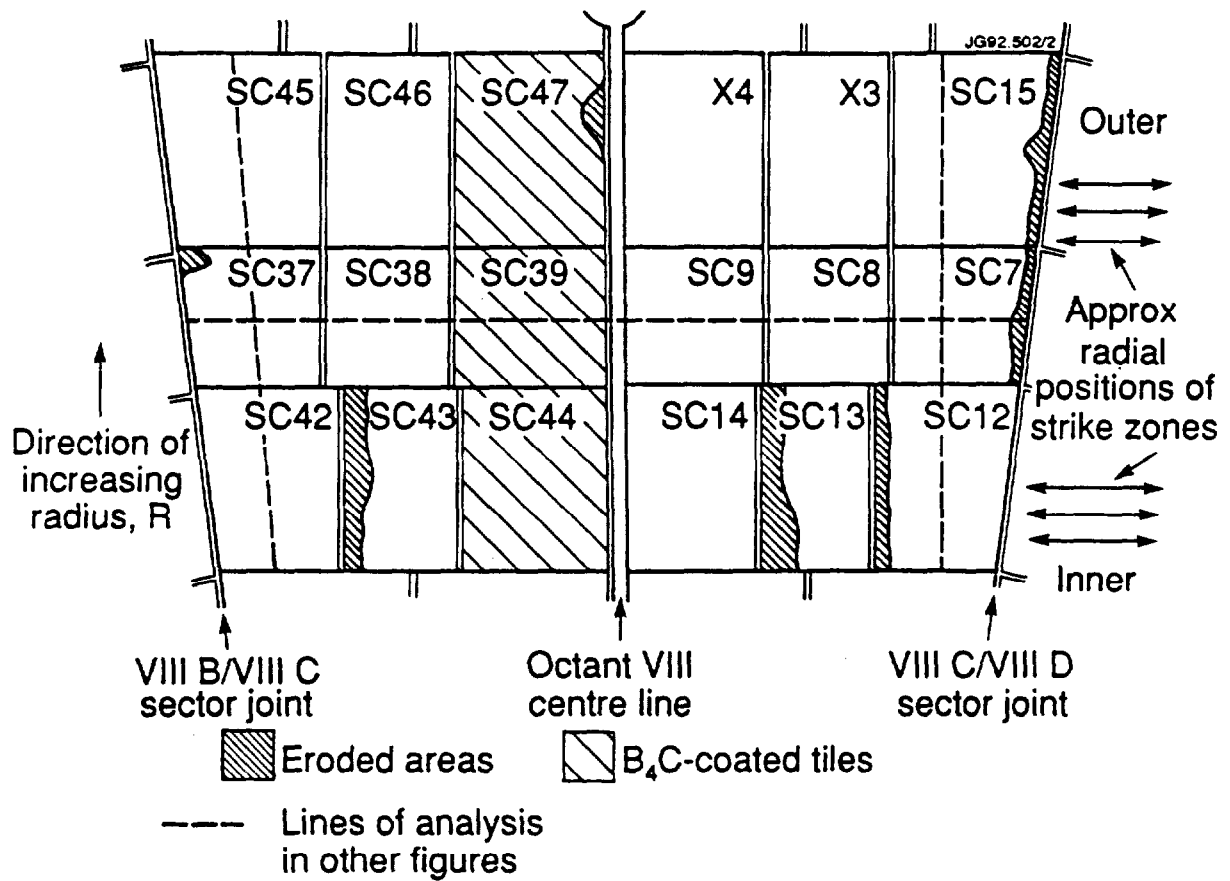Figure 1: Plan view of a sector of graphite tiles at the upper X-point region of the JET machine, showing the B₄C - coated tile positions.
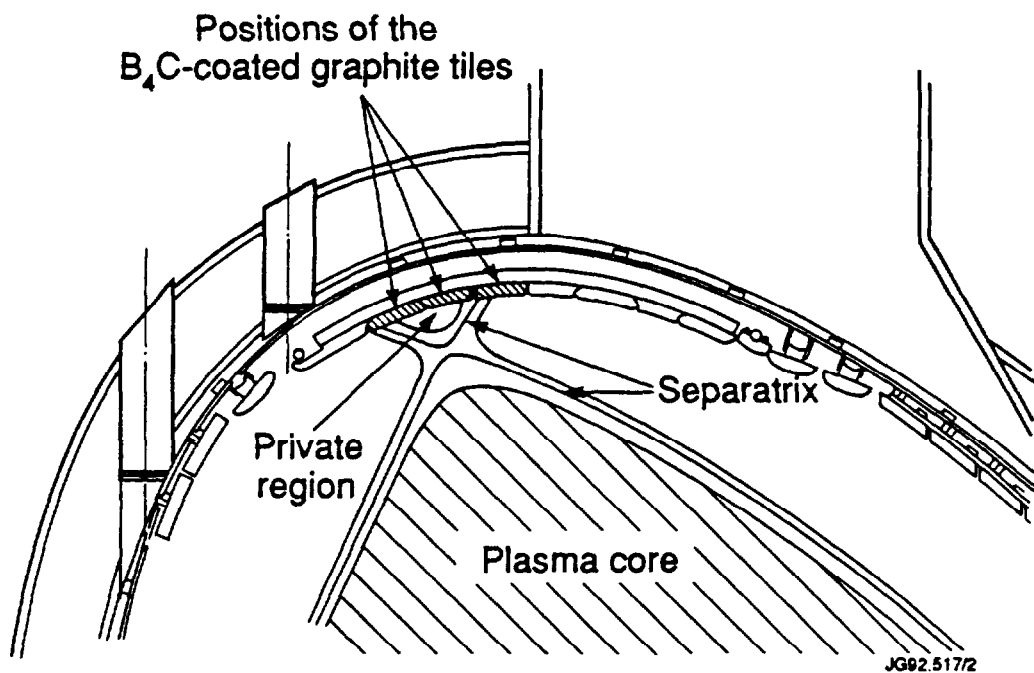


Figure 2: Diagram showing a part of the cross-section of JET containing the tiles shown in figure 1 and the relative plasma position.
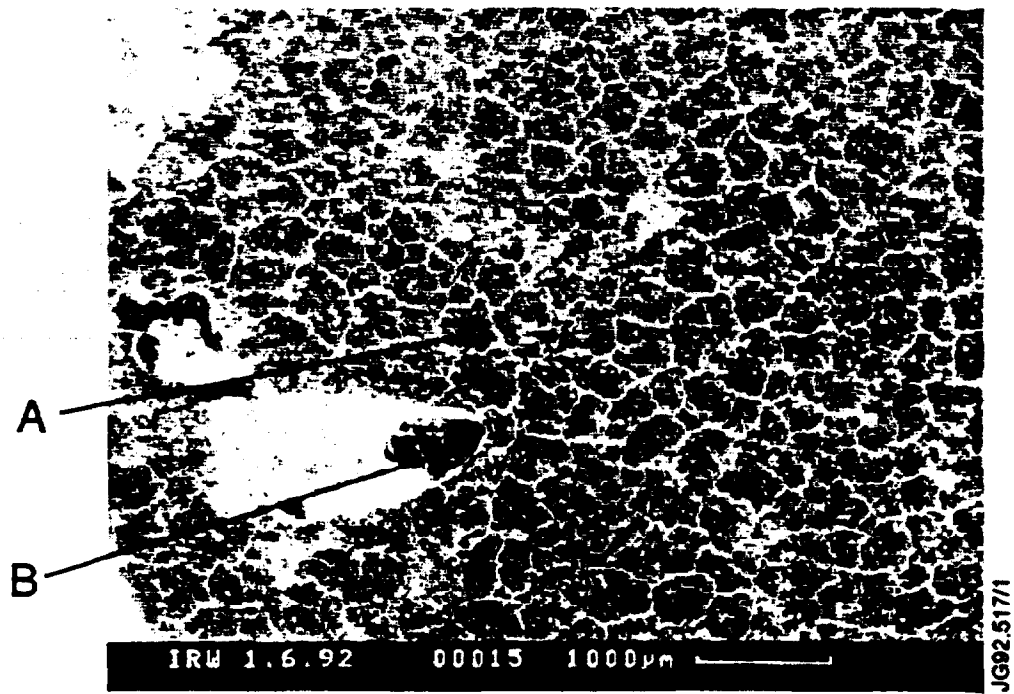
Figure 3: Secondary electron image of a small area of the surface of the coated tile SC47 after exposure in JET (taken from the central region).
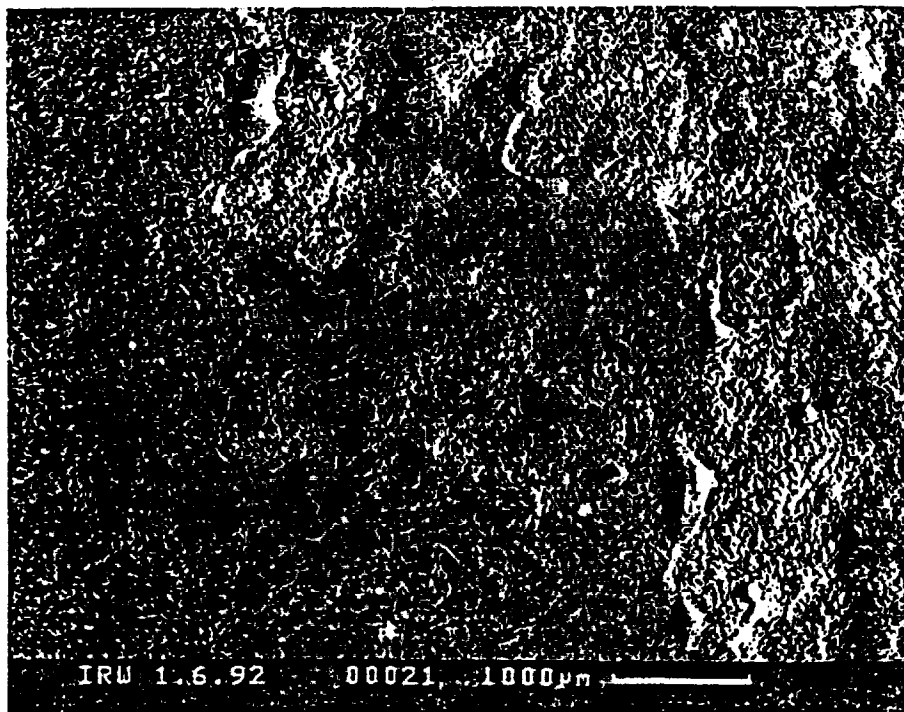


Figure 4: Another area in the central region of the coated tile SC47, imaged using back-scattered electrons.
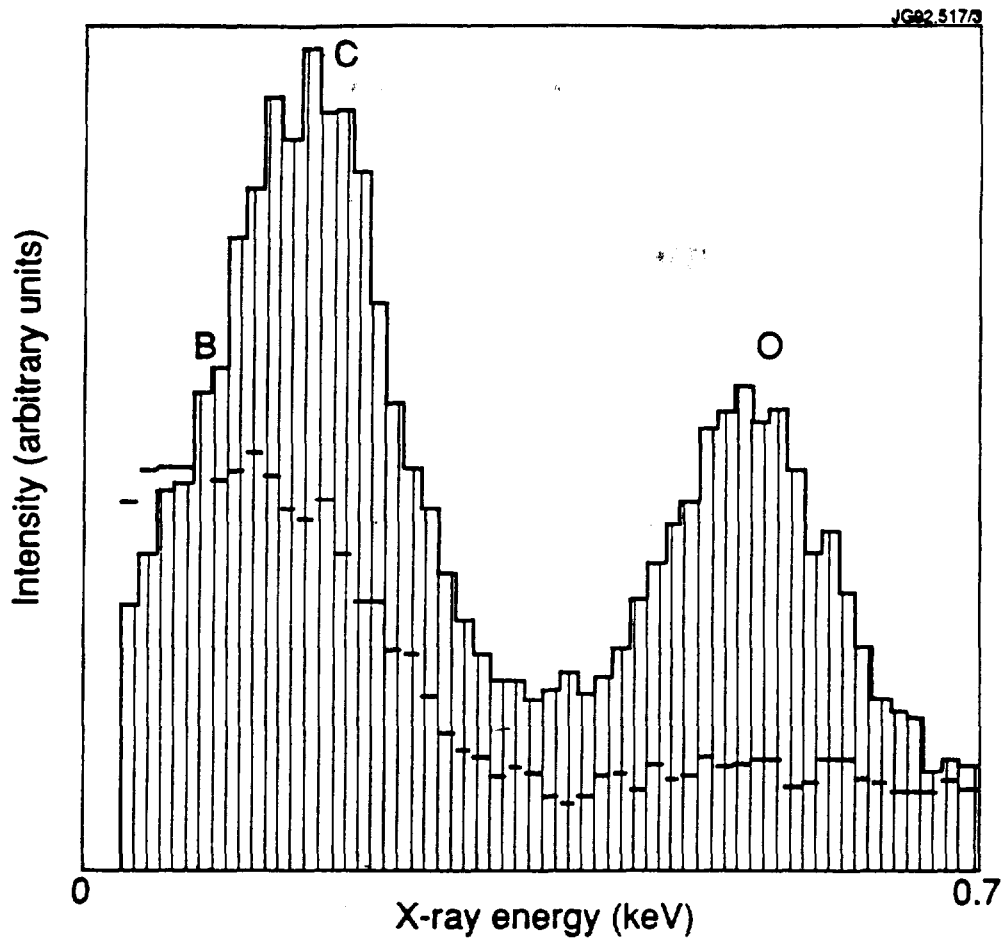
Figure 5: Low-energy part of the EDX spectra recorded from points A (full line and B (dashed line) on figure 3.
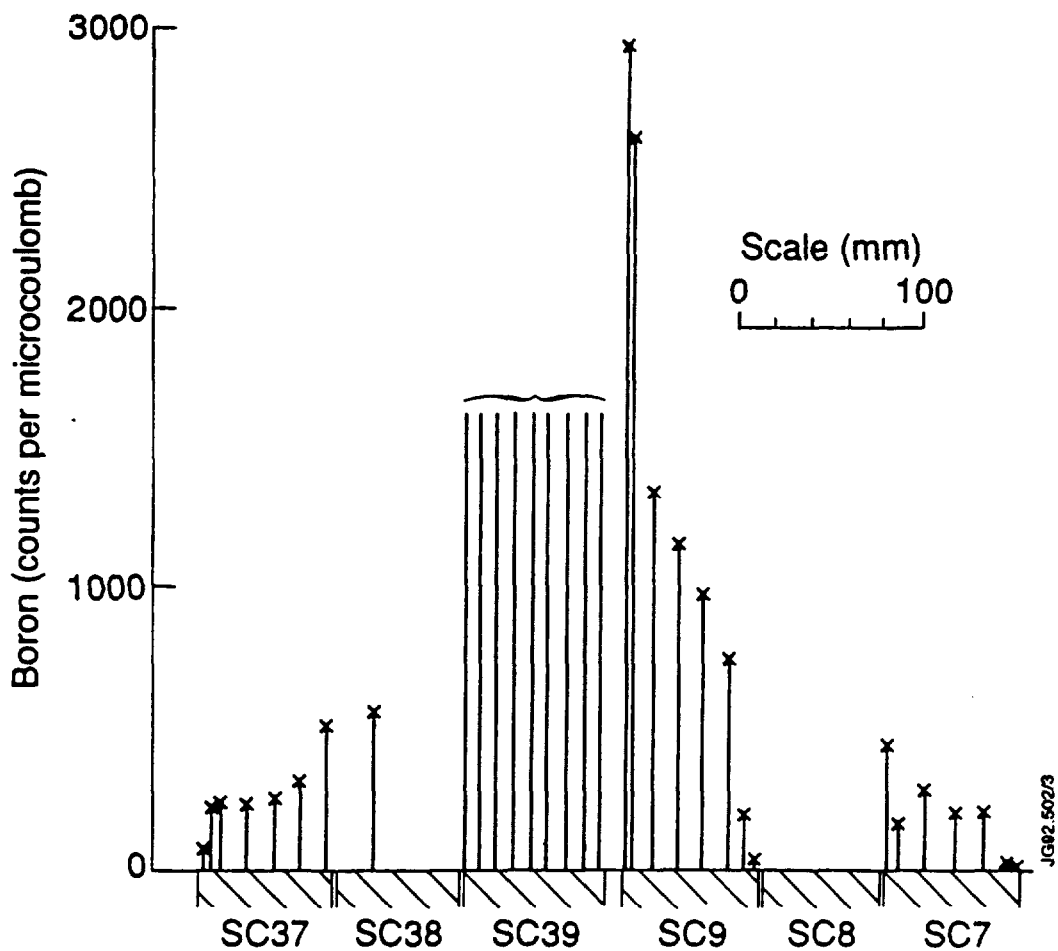


Figure 6: Boron concentration (in arbitrary units) at points along a toroidal line across the X-point (location of the line is shown in figure 1).
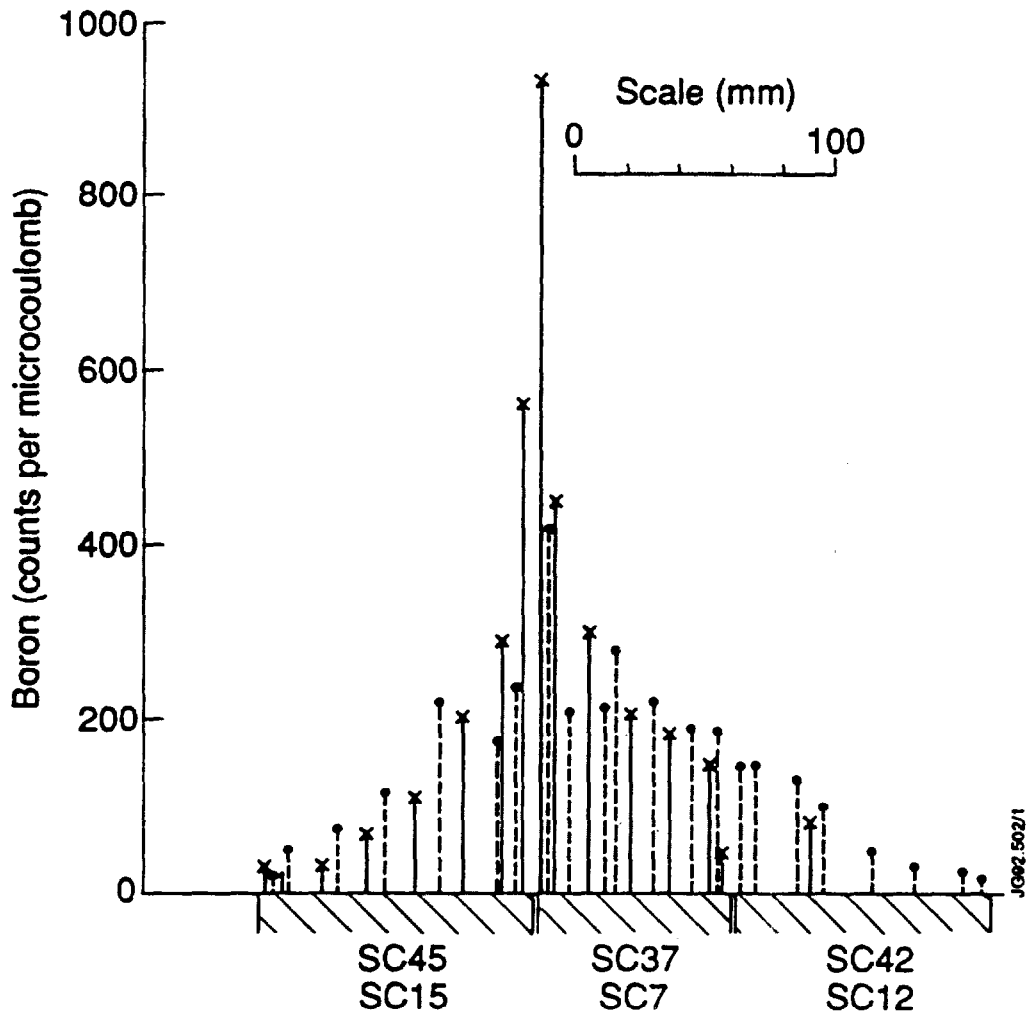
Figure 7: Boron concentrations (in arbitrary units) on the tiles at points along two poloidal lines across the X-point region. The full lines refer to points on tiles SC45, SC37 and SC42, the dashed lines to points on SC15, SC7 and SC12 (see also figure 1).

# Appendix I

## THE JET TEAM

JET Joint Undertaking, Abingdon, Oxon, OX14 3EA, U.K.

J.M. Adams[1], B. Alper, H. Altmann, A. Andersen[14], P. Andrew, S.Ali-Arshad, W. Bailey, B. Balet, P. Barabaschi, Y. Baranov, P. Barker, R. Barnsley[2], M. Baronian, D.V. Bartlett, A.C. Béll, G. Benali, P. Bertoldi, E. Bertolini, V. Bhatnagar, A.J. Bickley, D. Bond, T. Bonicelli, S.J. Booth, G. Bosia, M. Botman, D. Boucher, P. Boucquey, M. Brandon, P. Breger, H. Brelen, W.J. Brewerton, H. Brinkschulte, T. Brown, M. Brusati, T. Budd, M. Bures, P. Burton, T. Businaro, P. Butcher, H. Buttgereit, C. Caldwell-Nichols, D.J. Campbell, D. Campling, P. Card, G. Celentano, C.D. Challis, A.V.Chankin[23], A. Cherubini, D. Chiron, J. Christiansen, P. Chuilon, R. Claesen, S. Clement, E. Clipsham, J.P. Coad, I.H. Coffey[24], A. Colton, M. Comiskey[4], S. Conroy, M. Cooke, S. Cooper, J.G. Cordey, W. Core, G. Corrigan, S. Corti, A.E. Costley, G. Cottrell, M. Cox[7], P. Crawley, O. Da Costa, N. Davies, S.J. Davies[7], H. de Blank, H. de Esch, L. de Kock, E. Deksnis, N. Deliyanakus, G.B. Denne-Hinnov, G. Deschamps, W.J. Dickson[19], K.J. Dietz, A. Dines, S.L. Dmitrenko, M. Dmitrieva[25], J. Dobbing, N. Dolgetta, S.E. Dorling, P.G. Doyle, D.F. Düchs, H. Duquenoy, A. Edwards, J. Ehrenberg, A. Ekedahl, T. Elevant[11], S.K. Erents[7], L.G. Eriksson, H. Fajemirokun[12], H. Falter, J. Freiling[15], C. Froger, P. Froissard, K. Fullard, M. Gadeberg, A. Galetsas, L. Galbiati, D. Gambier, M. Garribba, P. Gaze, R. Giannella, A. Gibson, R.D. Gill, A. Girard, A. Gondhalekar, D. Goodall[7], C. Gormezano, N.A. Gottardi, C. Gowers, B.J. Green, R. Haange, A. Haigh, C.J. Hancock, P.J. Harbour, N.C. Hawkes[7], N.P. Hawkes[1], P. Haynes[7], J.L. Hemmerich, T. Hender[7], J. Hoekzema, L. Horton, J. How, P.J. Howarth[5], M. Huart, T.P. Hughes[4], M. Huguet, F. Hurd, K. Ida[18], B. Ingram, M. Irving, J. Jacquinot, H. Jaeckel, J.F. Jaeger, G. Janeschitz, Z. Jankowicz[22], O.N. Jarvis, F. Jensen, E.M. Jones, L.P.D.F. Jones, T.T.C. Jones, J-F. Junger, F. Junique, A. Kaye, B.E. Keen, M. Keilhacker, W. Kerner, N.J. Kidd, R. Konig, A. Konstantellos, P. Kupschus, R. Lässer, J.R. Last, B. Laundy, L. Lauro-Taroni, K. Lawson[7], M. Lennholm, J. Lingertat[13], R.N. Litunovski, A. Loarte, R. Lobel, P. Lomas, M. Loughlin, C. Lowry, A.C. Maas[15], B. Macklin, C.F. Maggi[16], G. Magyar, V. Marchese, F. Marcus, J. Mart, D. Martin, E. Martin, R. Martin-Solis[8], P. Massmann, G. Matthews, H. McBryan, G. McCracken[7], P. Meriguet, P. Miele, S.F. Mills, P. Millward, E. Minardi[16], R. Mohanti[17], P.L. Mondino, A. Montvai[3], P. Morgan, H. Morsi, G. Murphy, F. Nave[27], S. Neudatchin[23], G. Newbert, M. Newman, P. Nielsen, P. Noll, W. Obert, D. O'Brien, J. O'Rourke, R. Ostrom, M. Ottaviani, S. Papastergiou, D. Pasini, B. Patel, A. Peacock, N. Peacock[7], R.J.M. Pearce, D. Pearson[12], J.F. Peng[26], R. Pepe de Silva, G. Perinic, C. Perry, M.A. Pick, J. Plancoulaine, J-P. Poffé, R. Pohlchen, F. Porcelli, L. Porte[19], R. Prentice, S. Puppin, S. Putvinskii[23], G. Radford[9], T. Raimondi, M.C. Ramos de Andrade, M. Rapisarda[29], P-H. Rebut, R. Reichle, S. Richards, E. Righi, F. Rimini, A. Rolfe, R.T. Ross, L. Rossi, R. Russ, H.C. Sack, G. Sadler, G. Saibene, J.L. Salanave, G. Sanazzaro, A. Santagiustina, R. Sartori, C. Sborchia, P. Schild, M. Schmid, G. Schmidt[6], H. Schroepf, B. Schunke, S.M. Scott, A. Sibley, R. Simonini, A.C.C. Sips, P. Smeulders, R. Smith, M. Stamp, P. Stangeby[20], D.F. Start, C.A. Steed, D. Stork, P.E. Stott, P. Stubberfield, D. Summers, H. Summers[19], L. Svensson, J.A. Tagle[21], A. Tanga, A. Taroni, C. Terella, A. Tesini, P.R. Thomas, E. Thompson, K. Thomsen, P. Trevalion, B. Tubbing, F. Tibone, H. van der Beken, G. Vlases, M. von Hellermann, T. Wade, C. Walker, D. Ward, M.L. Watkins, M.J. Watson, S. Weber[10], J. Wesson, T.J. Wijnands, J. Wilks, D. Wilson, T. Winkel, R. Wolf, D. Wong, C. Woodward, M. Wykes, I.D. Young, L. Zannelli, A. Zolfaghari[28], G. Zullo, W. Zwingmann.

### PERMANENT ADDRESSES

1. UKAEA, Harwell, Didcot, Oxon, UK.
2. University of Leicester, Leicester, UK.
3. Central Research Institute for Physics, Budapest, Hungary.
4. University of Essex, Colchester, UK.
5. University of Birmingham, Birmingham, UK.
6. Princeton Plasma Physics Laboratory, New Jersey, USA.
7. UKAEA Culham Laboratory, Abingdon, Oxon, UK.
8. Universidad Complutense de Madrid, Spain.
9. Institute of Mathematics, University of Oxford, UK.
10. Freien Universität, Berlin, F.R.G.
11. Royal Institute of Technology, Stockholm, Sweden.
12. Imperial College, University of London, UK.
13. Max Planck Institut für Plasmaphysik, Garching, FRG.
14. Risø National Laboratory, Denmark.
15. FOM Instituut voor Plasmafysica, Nieuwegein, The Netherlands.
16. Dipartimento di Fisica, University of Milan, Milano, Italy.
17. North Carolina State University, Raleigh, NC, USA
18. National Institute for Fusion Science, Nagoya, Japan.
19. University of Strathclyde, 107 Rottenrow, Glasgow, UK.
20. Institute for Aerospace Studies, University of Toronto, Ontario, Canada.
21. CIEMAT, Madrid, Spain.
22. Institute for Nuclear Studies, Otwock-Swierk, Poland.
23. Kurchatov Institute of Atomic Energy, Moscow, USSR
24. Queens University, Belfast, UK.
25. Keldysh Institute of Applied Mathematics, Moscow, USSR.
26. Institute of Plasma Physics, Academica Sinica, Hefei, P. R. China.
27. LNETI, Savacem, Portugal.
28. Plasma Fusion Center, M.I.T., Boston, USA.
29. ENEA, Frascati, Italy.

At 1st July, 1992